Inorganic Chemistry
Article

Inorg. Chem. **2010**, *49*, 2715–2720 **2715**
DOI: 10.1021/ic901963t

Structure Determination and Relative Properties of Novel Chiral Orthoborate $KMgBO_3$

L. Wu,*,† J. C. Sun,† Y. Zhang,‡ S. F. Jin,§ Y. F. Kong,† and J. J. Xu†

†*The MOE key laboratory of weak-Light Nonlinear Photonics, School of Physics, Nankai University, Tianjin 300071, China,* ‡*Institute of Photo-electronic Thin Film Devices and Technology, Nankai University, Tianjin 300071, China, and* §*Beijing National Laboratory for Condensed Matter Physics, Institute of Physics, Chinese Academy of Sciences, P.O. Box 603, Beijing 100190, China*

Received October 5, 2009

A novel chiral orthoborate, $KMgBO_3$, has been successfully synthesized via a standard solid-state reaction, and the crystal structure has been determined from powder X-ray diffraction data. It crystallizes in the cubic chiral space group $P2_13$. Isolated $[BO_3]^{3-}$ anionic groups, which are the fundamental building units, are distributed around the ⟨111⟩ crystallographic direction in an axial C_3 symmetry, and the configuration of O_3 planes is helical, similar to the aplanar ClO_3 groups in $NaClO_3$, which indicates an optical activity in it and is validated by the circular dichroism spectrum. The chiral feature of the borate is unique, and because of the noncentrosymmetric structure, the compound exhibits nonlinear optical properties, which are validated by second harmonic generation powder measurement. It has a wide transparency, including the vacuum ultraviolet region. The relations between the structures of $KMgBO_3$ and $NaClO_3$ and structural conversion form $KMgBO_3$ to $NaMgBO_3$ are also discussed. The ionic radii, interatomic distance, and the rigid tilting of BO_3 groups are considered to be the main factors in the crystallization of different structures.

Introduction

A noncentrosymmetric structure is a prerequisite for a crystal to exhibit efficient bulk second-order nonlinear optical (NLO) effects that can be exploited in the fabrication of second-harmonic generator (SHG), electro-optical, and photorefractive devices used in optical communications and semiconductor large-scale integrated circuits.[1,2] In past decades, much effort has been made to search for useful NLO crystals,[3−9] and more and more noncentrosymmetric borates such as β-BaB_2O_4,[3] LiB_3O_5,[4] $Sr_2Be_2B_2O_7$,[5] and $K_2Al_2B_2O_7$[6] have been found to be very useful as NLO materials. Then inorganic borates became a focus of research for their variety of structure types, transparency to a wide range of wavelengths, high laser damage tolerance, and high optical quality as potential NLO materials.[1] A variety of BO atomic groups are considered to be a dominant factor in their physical properties, in particular the optical properties. Among the various anionic groups, the planar $[BO_3]^{3-}$ groups attract our attention. Because of highly localized valence electrons, low absorption (173 nm),[5] and anisotropic polarizability, some borates are likely to be good candidates for future birefringent and deep-UV nonlinear optical (NLO) materials. Therefore, we have investigated the systems $M_2O-M'O-B_2O_3$ (M = Li, Na, K; M′ = Mg, Ca, Sr, Ba) to search for such new useful optical materials with $[BO_3]^{3-}$ anionic groups. Thirteen new compounds,[10−16] including the promising birefringent crystal $NaMgBO_3$[16] and nonlinear borates

*Author to whom correspondence should be addressed. Tel. +86 22 23506257. Fax: +86 22 23505409. E-mail: lwu@nankai.edu.cn.

(1) Becker, P. *Adv. Mater.* **1998**, *10*, 979–992.
(2) Chen, C. T.; Ye, N.; Lin, J.; Jiang, J.; Zeng, W.; Wu, B. *Adv. Mater.* **1999**, *11*, 1071–1078.
(3) Chen, C. T.; Wu, B.; Jiang, A.; You, G. *Sci. China B* **1985**, *18*, 235–243.
(4) Chen, C. T.; Wu, Y.; Jiang, A.; Wu, B.; You, G.; Li, R.; Lin, S. *J. Opt. Soc. Am. B* **1989**, *6*, 616–621.
(5) Chen, C. T.; Wang, Y.; Wu, B.; Wu, K.; Zeng, W.; Yu, L. *Nature* **1995**, *373*, 322–324.
(6) Hu, Z.; Higashiyama, T.; Yoshimura, M.; Mori, Y.; Sasaki, T *Z. Kristallogr.* **1999**, *214*, 433–434.
(7) Pan, S. L.; Smit, J. P.; Watkins, B.; Marvel, M. R.; Stern, C. L.; Poeppelmeier, K. R. *J. Am. Chem. Soc.* **2006**, *128*, 11631–11634.
(8) Pan, S. L.; Smit, J. P.; Marvel, M. R.; Stampler, E. S.; Haag, J. M.; Baek, J.; Halasyamani, P. S.; Poeppelmeier, K. R. *J. Solid State Chem.* **2008**, *181*, 2087–2091.
(9) Kong, F.; Huang, S. P.; Sun, Z. M.; Mao, J. G.; Cheng, W. D. *J. Am. Chem. Soc.* **2006**, *128*, 7750–7751.
(10) Wu, L.; Chen, X. L.; Li, H.; He, M.; Dai, L.; Li, X. Z.; Xu, Y. P. *J. Solid State Chem.* **2004**, *177*, 1111–1116.
(11) Wu, L.; Wang, C.; Chen, X. L.; Li, X. Z.; Xu, Y. P.; Cao, Y. G. *J. Solid State Chem.* **2004**, *177*, 1847–1851.
(12) Wu, L.; Chen, X. L.; Li, H.; He, M.; Xu, Y. P.; Li, X. Z. *Inorg. Chem.* **2005**, *44*, 6409–6414.
(13) Wu, L.; Chen, X. L.; Li, X. Z.; Dai, L.; Xu, Y. P.; Zhao, M. *Acta Crystallogr. C* **2005**, *61*, i32–i34.
(14) Wu, L.; Chen, X. L.; Xu, Y. P.; Sun, Y. P. *Inorg. Chem.* **2006**, *45*, 3042–3047.
(15) Wu, L.; Chen, X. L.; Zhang, Y.; Kong, Y. F.; Xu, J. J.; Xu, Y. P. *J. Solid State Chem.* **2006**, *179*, 1219–1224.
(16) Wu, L.; Zhang, Y.; Kong, Y. F.; Sun, T. Q.; Xu, J. J.; Chen, X. L. *Inorg. Chem.* **2007**, *46*, 5207–5211.

Published on Web 02/18/2010

Table 1. Crystallographic Data, Experimental Details of X-Ray Powder Diffraction, and Rietveld Refinement Data for $K_{1-x}Na_xMgBO_3$ (x = 0, 0.1, 0.2)[a]

chemical formula	$KMgBO_3$	$K_{0.9}Na_{0.1}MgBO_3$	$K_{0.8}Na_{0.2}MgBO_3$
fw	122.22	120.93	119.55
cryst syst	cubic	cubic	cubic
space group	$P2_13$	$P2_13$	$P2_13$
a (Å)	6.83443(4)	6.82475(5)	6.82370(6)
volume (Å^3)	319.23(1)	317.88(1)	317.73(1)
Z	4	4	4
d_c (g cm^{-3})	2.543	2.527	2.499
diffractometer	X'Pert Pro, PANalytical	X'Pert Pro, PANalytical	X'Pert Pro, PANalytical
radiation type	Cu Kα	Cu Kα	Cu Kα
wavelength (Å)	1.5418	1.5418	1.5418
profile range (°2θ)	10.008−134.975	10.008−134.975	10.008−134.975
step size (°2θ)	0.017	0.017	0.017
number of observations (N)	7352	7352	7352
number of contributing reflections	248 (Kα1 + Kα2)	248 (Kα1 + Kα2)	248 (Kα1 + Kα2)
number of structure parameters (P_1)	10	11	11
number of profile parameters (P_2)	17	17	17
R_{Bragg} (%)	6.42	6.70	8.29
R_p (%)	6.49	6.79	7.07
R_{wp} (%)	8.70	9.11	9.50
R_{exp} (%)	5.08	5.46	5.10

[a] $R_p = \sum|y_{io} - y_{ic}|/\sum|y_{io}|$, $R_{wp} = [\sum w_i(y_{io} - y_{ic})^2/\sum w_i y_{io}^2]^{1/2}$, $R_{exp} = [(N - P_1 - P_2)/\sum w_i y_{io}^2]^{1/2}$.

$NaCa_4(BO_3)_3$, $KCa_4(BO_3)_3$, and $KSr_4(BO_3)_3$,[14] have been synthesized successfully. Their powder XRD patterns have been submitted for publication in the Powder Diffraction File (International Centre for Diffraction Data). Considering the structure conversion from centrosymmetric $NaSr_4(BO_3)_3$[12] to noncentrosymmetric $KSr_4(BO_3)_3$, it seems the K^+ plays a key role in the structure conversion. $NaMgBO_3$ has a big birefringence, but it is centrosymmetric. If the structure could be changed to noncentrosymmetric by replacing Na^+ with K^+, the relative compound would be more attractive. Then, a new compound, $KMgBO_3$, with a noncentrosymmetric structure was synthesized successfully. The structure has been determined by the SDPD (Structure Determination from Powder Diffraction) method. What makes the structure remarkable is that it crystallizes in the cubic system, which is very rare in borate (there are 28 267 cubic compounds records in Findit,[17] in which only 58 records are borates, considering different records for one compound). The structural character of borates is far from being closely packed, which would favor cubic symmetry. In borate, however, especially if the fundamental building unit is the anisotropically polarizable planar BO_3 group, cubic crystals can be expected only if the BO_3 groups are distributed in a particular manner. One case can be seen in $MM'_4(BO_3)_3$ (M = Li, M′ = Sr; M = Na, M′ = Sr, Ba), in which isolated $[BO_3]^{3-}$ anionic groups are perpendicular to each other, distributed along ⟨100⟩ directions.[12] In contrast to that, in the new synthesized borate, $KMgBO_3$, isolated $[BO_3]^{3-}$ groups are arranged around the ⟨111⟩ crystallographic direction in an axial C_3 symmetry. Also, it crystallizes in a chiral space group $P2_13$, with the peculiar helical configuration of the O_3 group planes in $KMgBO_3$ resembling the arrangement of the ClO_3 groups in $NaClO_3$.[18,19] In these space groups, not only the nonlinear optical effect but also the optical activity can be expected. The structure of $KMgBO_3$ is found to have a close relationship with that of $NaClO_3$ but is distinct from $NaMgBO_3$. The structural changes of $K_{1-x}Na_xMgBO_3$ ($0 \le x \le 1$) will also be discussed here in order to gain better insight into the structural chemistry of these compounds.

Experimental Section

Solid-State Syntheses. Polycrystalline samples were prepared by sintering at high temperatures through solid-state reactions with stoichiometric starting reagents of analytical purity, K_2CO_3, $NaCO_3$, $SrCO_3$, and H_3BO_3. The mixtures were preheated at 600 °C to decompose the carbonate by reaction-driven processes and eliminate the water and then were elevated to higher sintering temperature up to 710 °C. In between sintering steps, the samples were cooled and ground. The purity was characterized on a PANalytical powder X-ray diffractometer X'Pert Pro with Cu Kα radiation (40 kV, 40 mA) at room temperature.

Data Collection and Structure Determination. The data of $KMgBO_3$, $K_{0.9}Na_{0.1}MgBO_3$, and $K_{0.8}Na_{0.2}MgBO_3$ used for structure determination and Rietveld refinement were collected by a step scan mode with a step width of $2\theta = 0.017°$ and a sampling time of 1 s in the range of 10°−135° at room temperature. Additional technical details are given in Table 1. The diffraction pattern of $KMgBO_3$ was indexed using DICVOL91[20] and gave out a cubic unit cell with a = 6.8388(6) Å. On the basis of the systematic absence of $h00$ with $h = 2n + 1$, $0k0$ with $k = 2n + 1$, and $00l$ with $l = 2n + 1$, the possible space groups are $P2_13$ and $P4_232$. Because the latter has a higher symmetry, it was tested first. However, it did not give a satisfying result.

The whole pattern of $KMgBO_3$ was fitted using the Fullprof program[21] based on the Le Bail method[22] with the other possible space group $P2_13$. The final agreement factors converged to R_p = 6.19%, R_{wp} = 8.54%, and R_{exp} = 5.24%. A total of 124 independent $|F_{obs}|$ values were extracted. Lattice parameters were refined to be a = 6.83451(7) Å. The direct method was applied with the *SHELXL97* program package[23] to the extracted $|F_{obs}|$. According to the atom distances, three peaks listed in the E-map were likely to correspond to the correct

(17) *Findit*, version 1.4.6; Fachinformationszentrum: Karlsruhe, Germany; National Institute of Standards and Technology: Gaithersburg, U.S.A., 2009.
(18) Ramachandran, G. N.; Chandrasekaran, K. S. *Acta Crystallogr.* **1957**, *10*, 671–675.
(19) Bruke-Laing, M. E.; Trueblood, K. N. *Acta Crystallogr. B* **1977**, *33*, 2698–2699.
(20) Boultif, A.; Louer, D. *J. Appl. Crystallogr.* **1991**, *24*, 987–993.
(21) Rodriquez-Carvajal, J.; Fernadez-Diaz, M. T.; Martinez, J. L. *J. Phys.: Condens. Matter* **1991**, *3*, 3215–3234.
(22) Le Bail, A.; Duroy, H.; Fourquet, J. L. *Mater. Res. Bull.* **1988**, *23*, 447–452.
(23) Sheldrick, G. M. *SHELXS97*; *SHELXL97*; University of Göttingen: Göttingen, Germany, 1997.

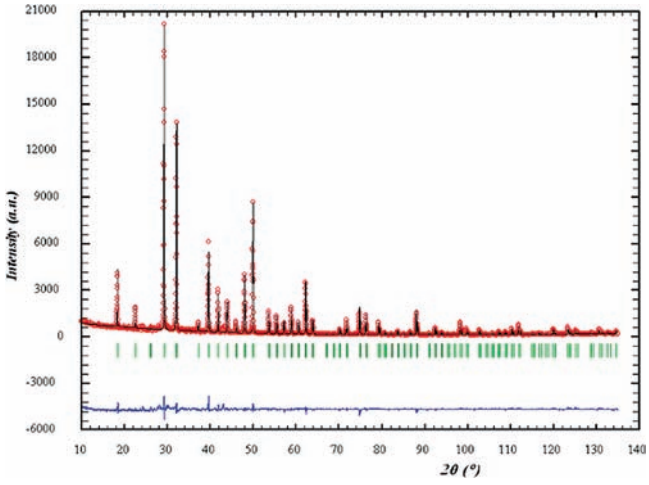

Figure 1. Final Rietveld refinement plots of $KMgBO_3$. Small circles (○) correspond to experimental values, and the continuous lines correspond to the calculated pattern; vertical bars (|) indicate the positions of Bragg peaks. The bottom trace depicts the difference between the experimental and the calculated intensity values.

positions of atoms. One of them was assigned to the K atom, and the other two peaks were assigned to Mg and B atoms, respectively. The O atom was located by using difference-Fourier synthesis. After the rough structure was obtained, a bond valence calculation[24] was used to check the consistency of the structure. Then, the structure was refined using the Rietveld method[25,26] within the Fullprof program. In the final cycle of refinement, a total of 27 parameters were refined (10 structural parameters and 17 profile parameters, including 5 background parameters and 5 peak-shape parameters; the pseudo-Voigt function was used as peak shape function), and the final agreement factors converged to R_B = 6.42%, R_p = 6.49%, R_{wp} = 8.70%, and R_{exp} = 5.08%. Lattice parameters were refined to be a = 6.83443(4)Å. The resulting structure was then put into the *PLATON* program package,[27] and no additional symmetry was found. The final refinement pattern is given in Figure 1. The crystallographic data, fractional atomic coordinates, and equivalent isotropic displacement parameters are reported in Tables 1 and 2; selected bond lengths and angles are listed in Table 3.

The structures of $K_{0.9}Na_{0.1}MgBO_3$ and $K_{0.8}Na_{0.2}MgBO_3$ (nominal composition) were refined by the Rietveld method. K^+ cations in $KMgBO_3$ are located in one crystallographic position (4*a*). It is coordinated by six oxygen atoms, which are also the vertices of BO_3 triangles. We suppose Na^+ cations statistically occupy the same sites as K^+. With the structure of $KMgBO_3$ as the starting model, Rietveld refinements were performed on the structures of $K_{0.9}Na_{0.1}MgBO_3$ and $K_{0.8}Na_{0.2}MgBO_3$. In the final cycle of refinement, a total of 28 parameters were refined (11 structural parameters and 17 profile parameters), and the final agreement factors converged to R_B = 6.70%, R_p = 6.79%, R_{wp} = 9.11%, and R_{exp} = 5.46% for $K_{0.9}Na_{0.1}MgBO_3$ and R_B = 8.29%, R_p = 7.07%, R_{wp} = 9.50%, and R_{exp} = 5.10% for $K_{0.8}Na_{0.2}MgBO_3$. Lattice parameters were refined to be a = 6.82475(6) Å for $K_{0.9}Na_{0.1}MgBO_3$ and a = 6.82370(6) Å for $K_{0.8}Na_{0.2}MgBO_3$. The final compositions were refined to be $K_{0.92}Na_{0.08}MgBO_3$ and $K_{0.83}Na_{0.17}MgBO_3$, respectively, which is in good agreement with the composition of the starting materials. Some important structural parameters are listed in Tables 1−3.

IR, UV−Vis, and CD Spectra Measurements. Infrared spectra were recorded with a 560E.S.P infrared spectrophotometer in the 400−2000 cm^{-1} wavenumber range using KBr pellets. The UV−visible absorption spectrum was measured at room temperature with a Hitachi U-4100 UV−visible spectrophotometer equipped with an integrating sphere in the absorption mode, which has a cutoff point at 185 nm. $BaSO_4$ is taken as the standard. The circular dichroism (CD) spectrum was measured on a JASCO J-715 spectropolarimeter in the range of 200−350 nm. The polycrystalline sample was mixed with KBr in a 1:20 ratio of $KMgBO_3$/KBr, and the KBr background was deducted.

Second-Harmonic Generation Measurement. A powder second-harmonic generation test was carried out on the $KMgBO_3$ sample by means of the Kurtz and Perry technique[28] with a Nd:YAG laser (1064 nm) as an incident light source. KDP was taken as the standard NLO material, and the ratio of the second-harmonic intensity outputs (532 nm) was calculated. The polycrystalline $KMgBO_3$ was ground and sieved into distinct particle size ranges, 15−31, 31−50, 50−74, 74−98, 98−125, and 125−180 μm, to test the variation of the SHG efficiencies with particle sizes.

Table 2. Fractional Atomic Coordinates and Equivalent Isotropic Displacement Parameters (Å^2) for $K_{1-x}Na_xMgBO_3$ (x = 0, 0.1, 0.2)

	site	x	y	z	U_{eq}	occupancy
			$KMgBO_3$			
Mg	4*a*	0.8542(2)	0.8542(2)	0.8542(2)	0.0072(1)	1.0000
K	4*a*	0.1344(1)	0.1344(1)	0.1344(1)	0.01454(7)	1.0000
O	12*b*	0.4153(1)	0.2576(1)	0.5376(1)	0.0105(1)	1.0000
B	4*a*	0.4002(1)	0.4002(1)	0.4002(1)	0.0301(5)	1.0000
			$K_{0.9}Na_{0.1}MgBO_3$			
Mg	4*a*	0.8553(2)	0.8553(2)	0.8553(2)	0.0050(1)	1.0000
K	4*a*	0.1342(2)	0.1342(2)	0.1342(2)	0.01260(7)	0.9196(4)
Na	4*a*	0.1342(2)	0.1342(2)	0.1342(2)	0.01260(7)	0.0804(4)
O	12*b*	0.4175(2)	0.2567(1)	0.5384(1)	0.0095(1)	1.0000
B	4*a*	0.4077(1)	0.4077(1)	0.4077(1)	0.0355(6)	1.0000
			$K_{0.8}Na_{0.2}MgBO_3$			
Mg	4*a*	0.8551(2)	0.8551(2)	0.8551(2)	0.0101(8)	1.0000
K	4*a*	0.1343(2)	0.1343(2)	0.1343(2)	0.00985(8)	0.8342(4)
Na	4*a*	0.1343(2)	0.1343(2)	0.1343(2)	0.00985(8)	0.1658(4)
O	12*b*	0.4172(2)	0.2582(2)	0.5413(2)	0.0174(2)	1.0000
B	4*a*	0.4084(2)	0.4084(2)	0.4084(2)	0.0524(8)	1.0000

Results and Discussion

Description of Crystal Structures. The $KMgBO_3$ compound crystallizes in the space group $P2_13$. As illustrated in Figure 2a and b, the foundational building units of $KMgBO_3$ are isolated planar $[BO_3]^{3-}$ anionic groups. The B−O bond lengths are 1.357(1) Å, and the O−B−O angles are 119.9(1)°, which is normal in a BO_3 plane triangle. The Mg, K, and B atoms are distributed along the normal directions of BO_3 planes, in three different 4*a* sites. The Mg atom is coordinated with six O atoms to form a distorted octahedron, as illustrated in Figure 3a. Those MgO_6 octahedra are edge-sharing with the adjacent BO_3 groups and vertex-sharing with each other to form the framework. There are six O atoms around the K atom (Figure 3b), forming a distorted octahedron. The KO_6 octahedra are connected to each other via one vertex and share one bridging oxygen with the adjacent planar BO_3 triangles. The MgO_6 and KO_6 distorted octahedra are joined together by vertex-sharing with bridging-oxygen atoms to form an infinite three-dimensional framework.

(24) Brown, I. D.; Altermatt, D. *Acta Crystallogr. B* **1985**, *41*, 244–247.
(25) Rietveld, H. M. *Acta Crystallogr.* **1967**, *22*, 151–152.
(26) Rietveld, H. M. *J. Appl. Crystallogr.* **1979**, *12*, 483–485.
(27) Spek, A. L. *J. Appl. Crystallogr.* **2003**, *36*, 7–13.
(28) Kurtz, S. K.; Perry, T. T. *J. Appl. Phys.* **1968**, *39*, 3798–3813.

Table 3. Selected Interatomic Distances (Å) and Angles (deg) for $K_{1-x}Na_xMgBO_3$ (x = 0, 0.1, 0.2)

$KMgBO_3$		$K_{0.9}Na_{0.1}MgBO_3$		$K_{0.8}Na_{0.2}MgBO_3$	
Mg−O^b	2.0919(19)	Mg−O^b	2.1084(18)	Mg−O^b	2.0951(22)
Mg−O^f	2.0919(18)	Mg−O^f	2.1084(18)	Mg−O^f	2.0951(22)
Mg−O^j	2.0919(18)	Mg−O^j	2.1084(17)	Mg−O^j	2.0951(21)
Mg−O^g	2.1531(18)	Mg−O^g	2.1332(18)	Mg−O^g	2.1510(22)
Mg−O^c	2.1531(19)	Mg−O^c	2.1332(18)	Mg−O^c	2.1510(21)
Mg−O^k	2.1531(18)	Mg−O^k	2.1332(18)	Mg−O^k	2.1510(21)
K−O^c	2.7808(16)	K(Na)−O^c	2.7694(15)	K(Na)−O^c	2.7749(18)
K−O^g	2.7808(18)	K(Na)−O^g	2.7694(17)	K(Na)−O^g	2.7749(21)
K−O^k	2.7808(16)	K(Na)−O^k	2.7694(16)	K(Na)−O^k	2.7749(20)
K−O^a	2.7948(17)	K(Na)−O^a	2.7809(16)	K(Na)−O^a	2.7624(19)
K−O^e	2.7948(16)	K(Na)−O^e	2.7809(15)	K(Na)−O^e	2.7624(20)
K−O^i	2.7948(17)	K(Na)−O^i	2.7809(16)	K(Na)−O^i	2.7624(20)
B−O	1.3570(14)	B−O	1.3648(14)	B−O	1.3700(17)
B−O^d	1.3570(15)	B−O^d	1.3648(14)	B−O^d	1.3700(18)
B−O^h	1.3570(15)	B−O^h	1.3648(15)	B−O^h	1.3700(19)
O−B−O^d	119.92(13)	O−B−O^d	119.91(13)	O−B−O^d	119.94(16)
O−B−O^h	119.92(13)	O−B−O^h	119.91(13)	O−B−O^h	119.94(17)
O^d−B−O^h	119.92(15)	O^d−B−O^h	119.91(14)	O^d−B−O^h	119.94(18)

^{a} $x+1/2, -y+1/2, -z$. ^{b} $-x, y+1/2, -z+1/2$. ^{c} $-x+1/2, -y, z+1/2$. ^{d} y, z, x. ^{e} $-y+1/2, -z, x+1/2$. ^{f} $y+1/2, -z+1/2, -x$. ^{g} $-y, z+1/2, -x+1/2$. ^{h} z, x, y. ^{i} $-z, x+1/2, -y+1/2$. ^{j} $-z+1/2, -x, y+1/2$. ^{k} $z+1/2, -x+1/2, -y$.

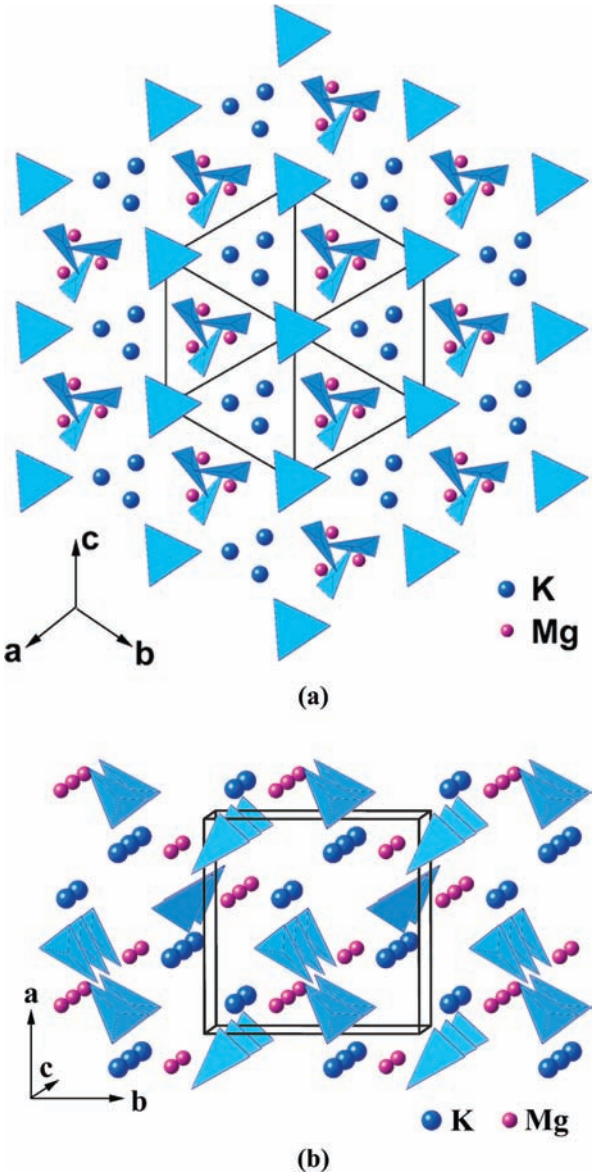

Figure 2. Structure projection of $KMgBO_3$ viewed along [111] (a) and [100] (b). The triangles are the planar BO_3 groups.

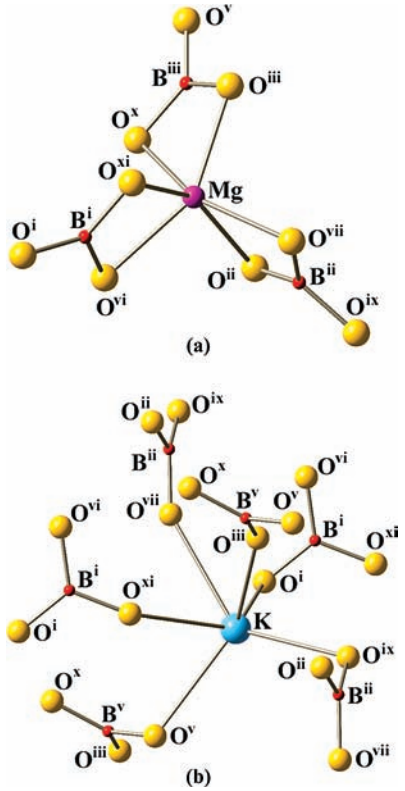

Figure 3. Coordination environments of Mg (a) and K (b) with O atoms. [symmetry code: (i) $x+1/2, -y+1/2, -z$; (ii) $-x, y+1/2, -z+1/2$; (iii) $-x+1/2, -y, z+1/2$; (iv) y, z, x; (v) $-y+1/2, -z, x+1/2$; (vi) $y+1/2, -z+1/2, -x$; (vii) $-y, z+1/2, -x+1/2$; (viii) z, x, y; (ix) $-z, x+1/2, -y+1/2$; (x) $-z+1/2, -x, y+1/2$; (xi) $z+1/2, -x+1/2, -y$.].

The overall structure of $KMgBO_3$ looks similar to that of $NaClO_3$, as presented in Figure 4. The K atoms are close to the corresponding positions of the Na atoms in $NaClO_3$, with a small movement along the normal directions of the BO_3 planes. A similar situation can also be found between B and Cl atoms, but the movement is going in an opposite way. The distance between K and B is shorter than that of Na and Cl. The Mg atoms occupy the third 4*a* position, which is empty in $NaClO_3$. It is found that the cations are distributed in the order of "...Mg−K−B−Mg−K−B..."

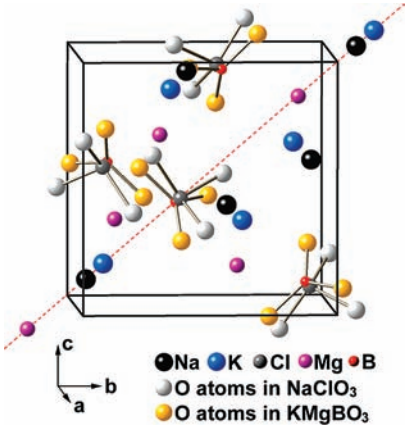

Figure 4. Comparison of the structures of $KMgBO_3$ and $NaClO_3$. The body diagonal is marked for clarity.

Table 4. Mg−O, K−O, and B−O Bond Valence in $KMgBO_3$[a]

	O	ΣS
Mg	0.340 × 3	1.884
	0.288 × 3	
K	0.173 × 3	1.020
	0.167 × 3	
B	1.039 × 3	3.117
ΣS	2.007	

[a] The summaries of bond valence for O only account for one of those numbers without being multiplied by 3, according to the coordination numbers.

along the normal directions of BO_3 planes, which might be one of the reasons why Na cannot be stabilized in the same site as K to form $NaMgBO_3$ with the same chiral structure. Comparing with K, Na has a smaller ionic radius, which is a disadvantage to keep a suitable distance between Mg and B without a change of the structure. Because the ionic radius of B is smaller than that of Cl, O atoms are bonded to the B atom at a shorter distance than Cl−O (1.485 Å), to form BO_3 triangles. Considering the same point group of 23, and the similar helical configuration of O_3 planes in $KMgBO_3$ and $NaClO_3$, optical activity will be realized in $KMgBO_3$.[29]

Bond Valence Calculation. To provide a check on the consistency of the structure determination, the bond valences have been calculated according to the Brown and Altermatt parameters[24] for the refined structure of $KMgBO_3$ and are listed in Table 4. It is obvious that the bond valence sums are reasonable for both cations and oxygens.

Infrared Spectra Analysis. To further confirm the coordination surroundings of B−O in the $KMgBO_3$ structure, the IR spectrum of it has been measured at room temperature and is shown in Figure 5. The IR absorption at wavenumbers smaller than 500 cm^{-1} mainly originates from the lattice dynamic modes. The strong band observed above 1200 cm^{-1} should be assigned to the $B-O_{external}$ stretching mode of triangular $[BO_3]^{3-}$ groups, while the bands with maxima at about 600−800 cm^{-1} should be attributed to the $B-O_{external}$ out of plane bending, which confirms the existence of the $[BO_3]^{3-}$ groups.[30]

(29) Glazer, A. M.; Stadnicka, K. *J. Appl. Crystallogr.* **1986**, *19*, 108–122.
(30) Rulmont, A.; Almou, M. *Spectrochim. Acta* **1989**, *45A*(5), 603–610.

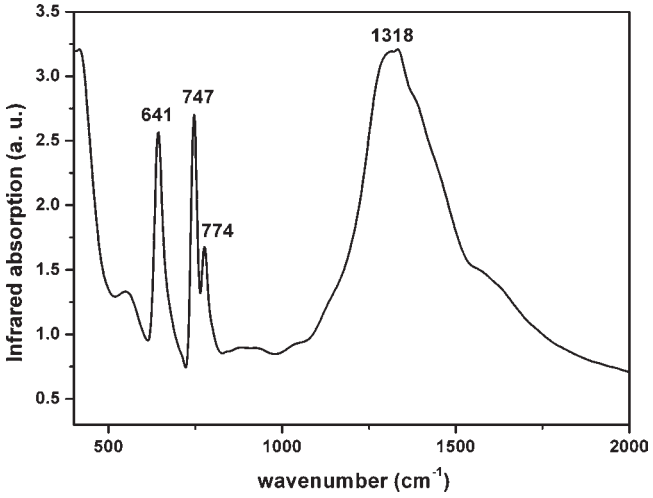

Figure 5. Infared spectrum of $KMgBO_3$.

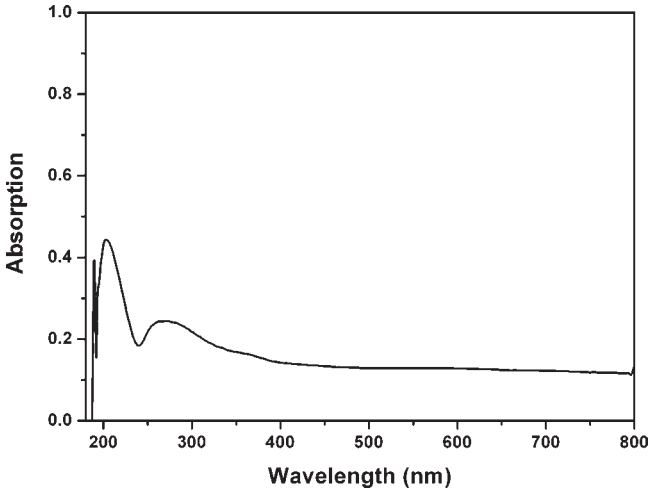

Figure 6. UV−visible absorption spectrum of $KMgBO_3$.

SHG, Ultraviolet Absorption, and Optical Activity. One preliminary measurement of the second-order nonlinear optical effect for the powder sample of the compound has been carried out via the Kurtz−Perry method at room temperature. The investigation proves properties associated with the determined space group, in particular, the lack of an inversion center. The intensity of the green light (frequency-doubled output, $\lambda = 532$ nm) produced by $KMgBO_3$ powder is about one-third of that produced by KDP powder, indicating that $KMgBO_3$ has a powder SHG effect smaller than that of KDP. The smaller SHG effect might be because of the helical configuration of BO_3 groups in $KMgBO_3$ counteracting partial anisotropy polarizability. It is found that the SHG intensities change slightly throughout the samples prepared with different particle sizes (Figure S1, Supporting Information). As an isometric crystal, $KMgBO_3$ is non-phase-matchable.[27] Although the intensity does not diminish consistently throughout the samples prepared with larger and larger particles, this is probably due to imperfect filtering allowing smaller particles to remain in the larger particle samples. The UV absorption spectrum of $KMgBO_3$ shows a weak absorption peak around 202 nm before the cutoff point of 185 nm of the spectrophotometer

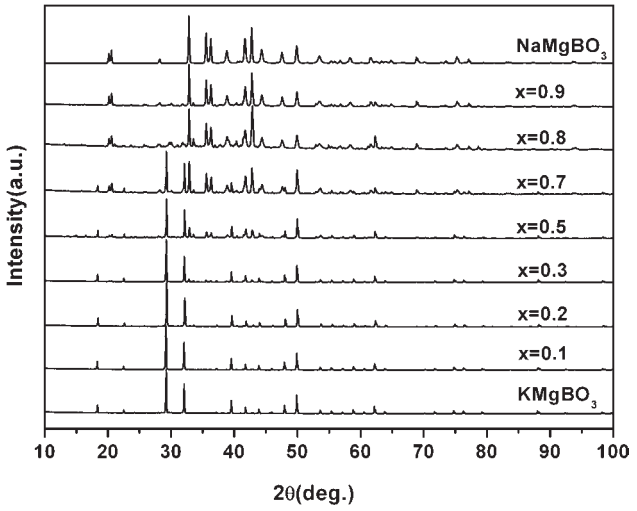

Figure 7. Powder X-ray diffraction patterns of $K_{1-x}Na_xMgBO_3$ ($0 \leq x \leq 1$) with different x values (x is the nominal Na content).

(Figure 6), which indicates it will also be transparent in the vacuum ultraviolet region. The circular dichroism spectrum collected from a polycrystalline $KMgBO_3$ sample shows several weak peaks of Cotton effects (Figure S2, Supporting Information), which can be easily repeated. Since the dextrorotatory and levorotatory enantiomers appear randomly, as a racemic mixture of the polycrystalline sample, the average intensity will be almost zero. The weak peaks should come from the random inequality of enantiomers in the polycrystalline sample, which confirm the optical activity of $KMgBO_3$.

Structural Changes of $K_{1-x}Na_xMgBO_3$ ($0 \leq x \leq 1$). It is interesting to find that the structure of $KMgBO_3$ has such a close relationship with that of $NaClO_3$, while $NaMgBO_3$ crystallizes in a completely different structure, although they have the same formula type of $ABCX_3$. No new structure type was observed in the pseudobinary system $KMgBO_3-NaMgBO_3$. However, a small homogeneous region was evidenced on the $KMgBO_3$ side. According to our powder X-ray diffraction measurements and Rietveld refinements, up to about 20% K^+ can be substituted by Na^+ with the structure type being retained (Figure 7). It is found that the lattice parameters and the calculated densities decrease with increasing Na content, reflecting the smaller radius and atomic weight of Na (Figure S3, Supporting Information). It is worth noticing that the bond lengths of K−O and B−O change in an opposite way. With increasing Na content, the K−O bond lengths decrease while the B−O bond length increases, and when the Na^+ is doped up to 17 atom %, the average B−O bond length is up to 1.370 (2) Å, almost equal to that in $NaMgBO_3$ (average value of 1.374 Å). Obviously, when a six-coordinated site is occupied by K, O atoms try to stay at sites far away from it to decrease the bond valence sum of K^+. On the other hand, Na^+ will try to keep O atoms around at smaller distances to increase the bond valence sum. The substitution of Na^+ for K^+ shortens the interatomic distance of K−O and enlarges that of B−O, which makes the structure of $KMgBO_3$ unstable. Since the BO_3 triangles are rather rigid, the lengthened B−O bonds tilt the BO_3 groups to a parallel distribution, as they are in $NaMgBO_3$; then the structure will change from $P2_13$ to $C2/c$. Even with the same coordination numbers of Mg, the surrounding-connected BO_3 groups of MgO_6 octahedra are different in $KMgBO_3$ and $NaMgBO_3$. Three BO_3 groups are edge-sharing with MgO_6 in $KMgBO_3$, while six BO_3 groups share corners with MgO_6 in $NaMgBO_3$. The coordination polyhedra of alkali metal cations are also different in the two compounds. Obviously, all of the difference comes from the different orientations of BO_3 planar triangles, which are helically distributed in $KMgBO_3$ and perfectly parallel in $NaMgBO_3$. The different arrangement modes of BO_3 groups lead to various structural types of alkali and alkaline-earth metal orthoborates, and many interesting properties.[12−16]

Conclusions

A novel chiral orthoborate $KMgBO_3$, was synthesized via a solid state reaction, and the structure was solved from powder X-ray diffraction data. Isolated planar $[BO_3]^{3-}$ anionic groups, which are the fundamental building units, are distributed in axial C_3 symmetry around the ⟨111⟩ crystallographic direction. Because of the similar helical configuration of O_3 planes to that of $NaClO_3$, an optical activity is realized in the title compound and characterized by the CD spectrum. The bond valence calculation, infrared spectra analysis, and second harmonic generation measurement were in good agreement with the crystallographic study and corroborate the validity of the structure. It was found that the smaller radius of Na might be the reason why $NaMgBO_3$ could not crystallize in the same chiral structure. On the other hand, the structural changes of $K_{1-x}Na_xMgBO_3$ ($0 \leq x \leq 1$) were studied. The ionic radii, interatomic distance, and especially the rigid tilting of BO_3 groups were believed to be the main factors controlling the structural conversion from $KMgBO_3$ to $NaMgBO_3$.

Acknowledgment. This work was financially supported by National Basic Research Program of China (2007CB307002), Chinese National Key Basic Research Special Fund (2006CB921703), Science Foundation of MOE for Doctoral Program (20070055096), Natural Science Foundation of Tianjin (09JCYBJC02500), and National Natural Science Foundation of China (50902074, 90922037 and 10774078). The work was also supported through a Grant-in-Aid from the International Centre for Diffraction Data (ICDD). We thank Mrs. Y. P. Xu of N01 group, Institute of Physics, Chinese Academy of Science; Mrs. Y. L. Wu of School of Chemistry; and Dr. J. W. Qi of Applied Physics School, Nankai University for their great help in collecting powder X-ray diffraction data and CD and UV−vis spectra measurements.

Supporting Information Available: Particle size vs SHG intensity data, CD spectrum, the variations of lattice parameters, calculated densities, bond lengths of K−O and B−O on the value of x in $K_{1-x}Na_xMgBO_3$ ($x = 0$, 0.1, 0.2), and crystallographic data in the CIF format for $KMgBO_3$, $K_{0.9}Na_{0.1}MgBO_3$, and $K_{0.8}Na_{0.2}MgBO_3$. This material is available free of charge via the Internet at http://pubs.acs.org.